Cellular/Molecular

TASK-2 Channels Contribute to pH Sensitivity of Retrotrapezoid Nucleus Chemoreceptor Neurons

Sheng Wang,[1,2]* Najate Benamer,[3,6]* Sébastien Zanella,[4]* Natasha N. Kumar,[1] Yingtang Shi,[1] Michelle Bévengut,[4] David Penton,[3,6] Patrice G. Guyenet,[1] Florian Lesage,[5,6] Christian Gestreau,[4]† Jacques Barhanin,[3,6]† and Douglas A. Bayliss[1]†

[1]Department of Pharmacology, University of Virginia School of Medicine, Charlottesville, Virginia 22908, [2]Department of Physiology, Hebei Medical University, Shijiazhuang, Hebei, 050017, China, [3]Université de Nice-Sophia Antipolis, Centre National de la Recherche Scientifique (CNRS), Laboratoire de PhysioMédecine Moléculaire (LP2M), Formation de Recherche en Evolution (FRE) 3472, Unité de Formation et de Recherche (UFR) Sciences, Parc Valrose, 06108 Nice, France, [4]Aix-Marseille-Université, CNRS, Centre de Recherche en Neurobiologie et Neurophysiologie de Marseille–Unité Mixte de Recherche (UMR) 7286, 13344 Marseille, France, [5]Université de Nice-Sophia Antipolis, CNRS, Institut de Pharmacologie Moléculaire, UMR7275, Sophia Antipolis, 06560 Valbonne, France, and [6]Laboratories of Excellence, Ion Channel Science and Therapeutics, France

Phox2b-expressing glutamatergic neurons of the retrotrapezoid nucleus (RTN) display properties expected of central respiratory chemoreceptors; they are directly activated by CO_2/H^+ via an unidentified pH-sensitive background K^+ channel and, in turn, facilitate brainstem networks that control breathing. Here, we used a knock-out mouse model to examine whether TASK-2 (K2P5), an alkaline-activated background K^+ channel, contributes to RTN neuronal pH sensitivity. We made patch-clamp recordings in brainstem slices from RTN neurons that were identified by expression of GFP (directed by the Phox2b promoter) or β-galactosidase (from the gene trap used for TASK-2 knock-out). Whereas nearly all RTN cells from control mice were pH sensitive (95%, $n = 58$ of 61), only 56% of GFP-expressing RTN neurons from *TASK-2*$^{-/-}$ mice ($n = 49$ of 88) could be classified as pH sensitive (>30% reduction in firing rate from pH 7.0 to pH 7.8); the remaining cells were pH insensitive (44%). Moreover, none of the recorded RTN neurons from *TASK-2*$^{-/-}$ mice selected based on β-galactosidase activity (a subpopulation of GFP-expressing neurons) were pH sensitive. The alkaline-activated background K^+ currents were reduced in amplitude in RTN neurons from *TASK-2*$^{-/-}$ mice that retained some pH sensitivity but were absent from pH-insensitive cells. Finally, using a working heart–brainstem preparation, we found diminished inhibition of phrenic burst amplitude by alkalization in *TASK-2*$^{-/-}$ mice, with apneic threshold shifted to higher pH levels. In conclusion, alkaline-activated TASK-2 channels contribute to pH sensitivity in RTN neurons, with effects on respiration *in situ* that are particularly prominent near apneic threshold.

Introduction

Central respiratory chemoreceptors sense CO_2/H^+ levels within the CNS and regulate the activity of the respiratory network to stabilize brain and arterial P_{CO_2}/pH at physiological levels. Several candidate cellular chemosensors have been identified within the caudal brainstem, but the molecular basis for CO_2/H^+ sensitivity has not been determined in any of those cell types (Nattie and Li, 2006; Guyenet et al., 2010; Feldman et al., 2013).

The Phox2b-expressing, glutamatergic neurons of the retrotrapezoid nucleus (RTN) have characteristics expected of central respiratory chemoreceptor neurons. These RTN neurons show a robust chemosensitivity, both *in vivo* and *in vitro* (Mulkey et al., 2004; Stornetta et al., 2006; Onimaru et al., 2012; Wang et al., 2013), and, when selectively activated by optogenetic approaches, RTN neurons stimulate breathing in anesthetized and conscious animals (Abbott et al., 2009, 2011; Kanbar et al., 2010). Conversely, inhibition or ablation of RTN neurons depresses ventilatory responses to CO_2 *in vivo* and raises the CO_2 threshold for breathing (Dubreuil et al., 2008; Takakura et al., 2008; Marina et al., 2010; Ramanantsoa et al., 2011). Moreover, the human condition of central congenital hypoventilation syndrome (CCHS), which is characterized by life-threatening defects in respiratory chemosensitivity, is attributable to a polyalanine expansion in the Phox2b transcription factor (Amiel et al., 2009; Carroll et al., 2010). Importantly, a mouse knock-in model that incorporates the human Phox2b mutation leads to selective ablation of glutamatergic neurons in RTN and complete disruption of the respiratory chemoreflex at birth (Dubreuil et al., 2008; Ramanantsoa et al., 2011).

Received June 9, 2013; revised July 26, 2013; accepted Aug. 5, 2013.

Author contributions: S.W., S.Z., N.N.K., Y.S., P.G.G., C.G., J.B., and D.A.B. designed research; S.W., N.B., S.Z., N.N.K., Y.S., and D.P. performed research; F.L. contributed unpublished reagents/analytic tools; S.W., N.B., S.Z., N.N.K., Y.S., M.B., P.G.G., F.L., C.G., J.B., and D.A.B. analyzed data; S.Z., N.N.K., P.G.G., C.G., J.B., and D.A.B. wrote the paper.

This work was supported by National Institutes of Health Grants HL74011 (P.G.G.) and HL108609 (D.A.B.) and French National Agency for Research Grants ANR RESPITASK (J.B., C.G.) and ANR-11-LABX-0015-01 (J.B., .F.L.).

*S.W., N.B., and S.Z. contributed equally to this work.

†C.G., J.B., and D.A.B. contributed equally to this work.

This article is freely available online through the *J Neurosci* Author Open Choice option.

Correspondence should be addressed to one of the following: Christian Gestreau, Aix Marseille Université, CNRS, CRN2M-UMR7286, 13344 Marseille Cedex 15, Marseille, France, E-mail: christian.gestreau@univ-amu.fr; Jacques Barhanin, Université de Nice-Sophia Antipolis, CNRS, Laboratoire de PhysioMédecine Moléculaire (LP2M), FRE 3472, UFR Sciences, Parc Valrose, 06108 Nice Cedex, France, E-mail: jacques.barhanin@unice.fr; or Douglas A. Bayliss, Department of Pharmacology, 1340 Jefferson Park Avenue, University of Virginia School of Medicine, Charlottesville, VA 22908, E-mail: bayliss@virginia.edu.

DOI:10.1523/JNEUROSCI.2451-13.2013

 0270-6474/13/3316033-12$15.00/0

The RTN neurons possess an intrinsic chemosensitivity that is attributable, at least in part, to a pH-sensitive background K^+ current (Mulkey et al., 2004; Lazarenko et al., 2009; Wang et al., 2013). Pharmacological experiments and studies using knock-out mice appear to exclude TASK-1 and TASK-3 channels (K2P3 and K2P9), two acid-sensitive members of the two-pore domain (K2P) family of background K^+ channels initially proposed for this role (Mulkey et al., 2007). Strikingly, a different member of the K2P family, the alkaline-activated TASK-2 channel (K2P5), is expressed in the RTN neurons that are selectively lost in mice bearing the CCHS mutation (Gestreau et al., 2010). In addition, TASK-2 knock-out mice presented with a blunted ventilatory response to CO_2, although measurements of pH-sensitive K^+ currents in RTN neurons were not provided (Gestreau et al., 2010).

Here, we used patch-clamp electrophysiology, histochemistry, single-cell RT-PCR (scPCR), and an *in situ* working heart–brainstem preparation to test directly the effect of TASK-2 channel deletion on the pH sensitivity of individual Phox2b-expressing RTN neurons and on CO_2 modulation of central respiratory output. We found that TASK-2 channels indeed contribute to pH sensitivity in Phox2b-expressing RTN neurons, and they are fully responsible for the pH-sensitive background K^+ current in nearly half of those cells. The diminished RTN neuronal pH sensitivity was reflected in blunted effects of lowering CO_2 on central respiratory drive in an *in situ* preparation from *TASK-2*$^{-/-}$ mice, and a correspondingly higher pH level was required to eliminate respiratory neural output. Thus, TASK-2 channels represent a molecular substrate for pH sensing in RTN respiratory chemoreceptor neurons.

Materials and Methods

Animals of either sex were used for all experiments in accordance with Animal Care and Use Guidelines from the National Institutes of Health and in accordance with French national legislation (Directive JO 87-848) and the European Communities Council (Directive 2010/63/EU, 74). All animal protocols were approved by either the Animal Care and Use Committee of the University of Virginia or the local ethics committee Direction Départementale de la Protection des Populations, Préfecture des Bouches du Rhône (with permit numbers 13-06 and 13-227 delivered to M.B. and C.G., respectively). Animals had access to food and water *ad libitum* and were exposed to 12 h light/dark cycles.

TASK-2 Knockout and Phox2b–GFP mice. We used previously described TASK-2 knock-out mice and a BAC transgenic mouse line to characterize effects of TASK-2 deletion on pH sensitivity in the Phox2b-expressing population of RTN neurons. The TASK-2 knock-out line was provided by K. Mitchell and W. C. Skarnes (University of California, Berkeley, Berkeley, CA) and backcrossed onto the C57BL6/J genetic background for 10 generations (Gestreau et al., 2010). The mice were generated using an exon trapping approach in which the exon trap incorporated a β-galactosidase expression construct into the TASK-2 locus (Leighton et al., 2001), allowing localization of TASK-2 expression by staining for β-galactosidase enzyme activity. For some experiments, the TASK-2 knock-out mice were crossed with a line of BAC transgenic mice, produced by the GENSAT (Gene Expression Nervous System Atlas) group, in which GFP expression is directed selectively to Phox2b-expressing neurons (Lazarenko et al., 2009). The derivation and salient properties of these so-called Jx99 mice have been described previously (Lazarenko et al., 2009). In short, virtually all GFP-expressing RTN neurons in these mice express Phox2b, a marker for respiratory chemosensitive neurons (Lazarenko et al., 2009). Moreover, we find that ~95% of GFP-expressing neurons recorded from the RTN in brainstem slices from these mice are pH sensitive (Lazarenko et al., 2009). By crossing these two lines to obtain *TASK2–Jx99* mice, we could use GFP expression to identify RTN chemoreceptor neurons in a manner that does not rely on either TASK-2 expression or pH-dependent functional properties.

Electrophysiological recordings in brainstem slices. Transverse brainstem slices were prepared from neonatal mouse pups (P4–P12) after rapid decapitation, either with or without anesthesia (ketamine and xylazine at 375 and 25 mg/kg, i.m.). Brainstems were removed, and slices (300 μm) were cut in the coronal plane with a vibrating microslicer (DSK 1500E, Dosaka or Vibratome, Microm) in ice-cold sucrose-containing solution (in mM: 260 sucrose, 3 KCl, 5 $MgCl_2$, 1 $CaCl_2$, 1.25 NaH_2PO_4, 26 $NaHCO_3$, 10 glucose, and 1 kynurenic acid) or in artificial CSF (aCSF) solution (in mM: 118 NaCl, 6 KCl, 1.25 NaH_2PO_4, 25 $NaHCO_3$, 2 $CaCl_2$, 1 $MgCl_2$, and 25 glucose). Slices were incubated for 30 min to 1 h at 37°C and subsequently at room temperature in aCSF (described above) or in normal Ringer's solution containing the following (in mM): 130 NaCl, 3 KCl, 2 $MgCl_2$, 2 $CaCl_2$, 1.25 NaH_2PO_4, 26 $NaHCO_3$, and 10 glucose. All cutting and incubation solutions were bubbled with 95% O_2 and 5% CO_2.

We targeted RTN neurons for patch-clamp recordings from coronal brainstem slices in chambers on fixed-stage fluorescence microscopes equipped with infrared Nomarski optics (Carl Zeiss AxioExaminer and Olympus Optical BX51WI). RTN neurons were identified either by GFP expression (in the *TASK2–Jx99* line) or by use of fluorescein di-β-D-galactopyranoside (20 μM FDG; Sigma), a fluorogenic substrate for β-galactosidase activity (in the TASK-2 modified lines). For recordings, slices were superfused with either (1) HEPES-based buffer (in mM: 140 NaCl, 3 KCl, 2 $MgCl_2$, 2 $CaCl_2$, 10 HEPES, 10 glucose, with pH adjusted between 7.0 and 8.0 by addition of HCl or NaOH) or (2) HCO_3^--buffered aCSF in which solutions were bubbled with 85% O_2 and 5% CO_2 (balance N_2) to attain a pH of 7.4, with acidosis (pH 7.1) and alkalosis (pH 7.6) obtained by raising or decreasing CO_2 to 10 or 3%, respectively.

Recordings were performed in either cell-attached or whole-cell configurations at room temperature using pClamp, a Multiclamp amplifier, and a Digidata 1440A analog-to-digital converter (all from Molecular Devices) or the Patchmaster and Fitmaster programs and an EPC9 amplifier (all from HEKA Elektronik). Borosilicate patch electrodes (3–6 MΩ) were filled with the following (in mM): 120 KCH_3SO_3 (or KCl), 4 NaCl, 1 $MgCl_2$, 0.5 $CaCl_2$, 10 HEPES, 10 EGTA, 3 Mg-ATP, and 0–0.3 GTP-Tris, pH adjusted to 7.2 with KOH. All recordings were made in the presence of strychnine (1–30 μM), bicuculline (10–20 μM), and 6-cyano-7-nitroquinoxaline-2,3-dione (10–20 μM) in the bath solution to block fast excitatory and inhibitory synaptic transmission.

Cell-attached recordings of RTN neuronal firing were made under voltage clamp at a holding potential of −60 mV (Perkins, 2006), and recordings of membrane potential and action potential discharge were obtained by whole-cell current clamp (Mulkey et al., 2004; Lazarenko et al., 2009, 2010). Firing rate histograms were generated by integrating action potential discharge in 10 s bins using Spike2 software (Cambridge Electronic Design). We determined pH sensitivity of individual RTN neurons by plotting firing rate versus bath pH and calculating the pH value at which firing rate was reduced to half of that obtained at pH 7.0 (pH_{50}) using linear regression analysis (Excel) (Lazarenko et al., 2009). The pH-sensitive currents in RTN neurons were characterized under whole-cell voltage clamp; compensation for series resistance and cell capacitance was obtained using the amplifier circuits. We obtained steady-state current–voltage (I–V) relationships from a holding potential of −60 mV under control conditions and after bath acidification or alkalization (Mulkey et al., 2004); in some cases, tetrodotoxin (0.1 μM), 4-aminopyridine (10 mM), tetraethylammonium (3 mM), and barium (10 μM) were added to the bath. The I–V curve of the pH-sensitive current was obtained in individual cells by digital subtraction, normalized to cell capacitance (from the amplifier circuit), and averaged for presentation.

Working heart–brainstem or "in situ" *preparation.* The arterially perfused working heart–brainstem or "*in situ*" preparation of mice (P30–P40) was used as described previously (Paton, 1996; Gestreau et al., 2005; Stettner et al., 2008). In this preparation, the brainstem is well oxygenated, has a normal pH, and generates a eupneic pattern of respiratory motor activity (Dutschmann et al., 2000; Wilson et al., 2001). Mice were deeply anesthetized with isoflurane (1-chloro-2,2,2-trifluoroethyl-difluoromethylether; Baxter). Once respiration was depressed and the ani-

mal ceased to respond to noxious pinch to the tail or a hindpaw, it was transected below the diaphragm, decerebrated at the precollicular level, and transferred into an ice-cooled (5°C) aCSF (see below for composition) that was equilibrated with 95% O_2 and 5% CO_2. The skin and the lungs were removed. The left phrenic nerve was separated and cut at the level of the diaphragm and prepared for recording. The preparation was then transferred to a recording chamber. The descending aorta was cannulated and perfused with aCSF at 30°C containing the following (in mM): 125 NaCl, 3 KCl, 1.25 KH_2PO_4, 2.5 $CaCl_2$, 1.25 $MgSO_4$, 25 $NaHCO_3$, and 10 D-glucose (1.25% Ficoll) using a peristaltic pump (Watson-Marlow). The perfusate was oxygenated, and the pH was maintained at 7.35 by gassing the aCSF with a 90% O_2 and 5% CO_2 (balance nitrogen). The perfusate was filtered and passed through bubble traps to remove gas bubbles. The perfusate leaking from the preparation was collected and recirculated after reoxygenation. Cardiac activity returned within seconds and rhythmic contractions of respiratory muscles within a few minutes after onset of reperfusion. Respiratory-related movements were abolished by injecting 250 μl of saline (intravenous) containing vecuronium bromide (30 μg/ml; Organon). After paralysis, the perfusion flow was adjusted to obtain a clearly identifiable three-phase respiratory pattern. The preparations were deemed stable if such respiratory pattern was maintained for at least 30 min. Flow rates were 16–22 ml/min, and they generated a perfusion pressure of 40–70 mmHg as measured through a double lumen catheter connected to the aortic perfusion cannula.

Respiratory motor nerve activity was recorded from the central end of the phrenic nerve via a suction electrode. The activity was amplified (2000–10,000), filtered (0.1–3 kHz), rectified, and integrated (time constant of 100 ms). All data were digitized (sampling rate of 10 kHz) using a Digidata interface and stored on a computer using pClamp 10 software (Molecular Devices).

To test the chemosensitive response of the *in situ* preparations from mice, the levels of CO_2 were either increased or decreased from the control level of 5% producing changes in the pH but not in the O_2 level (90% in the gas mixture) using a gas mixer (CWE). The gas levels were controlled by using a gas analyzer (Golf120; Vigaz). The following tests were used: (1) hypercapnic acidic aCSF equilibrated with 7% CO_2, pH 7.2, or 9% CO_2, pH 7.1, as a model for respiratory acidosis; and (2) hypocapnic alkaline aCSF equilibrated with 3% CO_2, pH 7.55, or 2% CO_2, pH 7.8, as a model for respiratory alkalosis. In some cases, levels of CO_2 were decreased as low as 0.9%, pH 8.35, to determine the apneic threshold. To assess breathing activity, phrenic inspiratory burst frequency (cycles per minutes) and amplitude (relative to amplitude at 9% CO_2) were determined during the last minute of the control period and each test. Several tests were run in each preparation with order randomized to avoid time-dependent effects.

Histochemical analysis of TASK-2 expression. Localization of TASK-2 expression was examined in Phox2b-expressing RTN neurons of the *TASK2–Jx99* line by staining for β-galactosidase activity (from the TASK-2 gene trap construct) and immunohistochemistry for GFP (from the Phox2b BAC transgene) (Lazarenko et al., 2009; Gestreau et al., 2010); we also costained for tyrosine hydroxylase (TH) to distinguish RTN chemoreceptor neurons from nearby Phox2b-expressing C1 adrenergic neurons (Stornetta et al., 2006). Young (P11–P24) wild-type (*TASK-2*$^{+/+}$*–Jx*) and TASK-2 knock-out (*TASK-2*$^{-/-}$*–Jx*) mice were deeply anesthetized with ketamine and xylazine (200 and 14 mg/kg, i.p.) and perfused transcardially with PBS (0.1 M), pH 7.4, followed by 4% paraformaldehyde (in 0.1 M phosphate buffer, pH 7.4). The brain was drop-fixed for 1 h and then sectioned (30 μm; 1:3 series) with a vibrating microtome (VT1000S; Leica). Free-floating brainstem sections were stained with 5-bromo-4-chloro-3-indolyl-β-D-galactopyranoside (X-gal) for 24 h at 37°C, as described previously (Gestreau et al., 2010). Thereafter, the tissue was blocked for 1 h in Tris-buffered saline (TBS) containing 10% normal horse serum (NHS), 0.3% Triton X-100, and 0.05% merthiolate. Tissue sections were incubated for 48 h at 4°C with primary antibodies [chicken anti-GFP (1:1000; GFP-1020; Aves Labs) and sheep anti-TH (1:1000; AB1542; Millipore)] diluted in TBS containing 1% NHS, 0.1% Triton X-100, and 0.05% merthiolate. The sections were rinsed with TBS and incubated for 1 h with donkey anti-sheep Cy3 and donkey anti-chicken Alexa Fluor 488 (1:400; Jackson ImmunoResearch) in secondary buffer (1% NHS/TBS). Sections were mounted using Vectashield mounting media (Vector Laboratories) and viewed under bright-field (X-gal) and epifluorescence (GFP, TH) optics using a Z.1 Axioimager (Carl Zeiss) with a computer-controlled stage (Neurolucida software version 10; MicroBrightField Bioscience). The rostrocaudal distribution of GFP-positive (GFP$^+$), TH$^+$, and X-gal$^+$ neurons in the RTN region was mapped for each tissue section, and the population of putative chemoreceptor RTN neurons [i.e., GFP$^+$, non-catecholaminergic, TH-negative (TH$^-$) neurons] was identified within the marginal layer ventrolateral to the facial motor nucleus (Stornetta et al. 2006). To combine data across mice, tissue sections were aligned relative to the most rostral section containing the inferior olivary nucleus and the genu of the facial nerve (according to Paxinos and Franklin, 2004). The rostrocaudal distribution of GFP$^+$ and X-gal$^+$ neurons was mapped, and the proportion of GFP$^+$/TH$^-$ RTN neurons that were also X-gal$^+$ was quantified using NeuroExplorer software (MicroBrightField Bioscience).

scPCR from acutely dissociated GFP-expressing RTN neurons. Neurons were acutely dissociated from neonatal (P7–P10) brainstem slices prepared from Jx99 *Phox2b-GFP* mice, essentially as described previously (Wang et al., 2013). In short, transverse brainstem slices were prepared as described above and incubated for 15 min at room temperature in PIPES buffer (in mM: 120 NaCl, 5 KCl, 1 $CaCl_2$, 1 $MgCl_2$, 25 D-glucose, 20 PIPES, 100% O_2; Kay and Wong, 1986) and then for 60 min at 33°C in PIPES containing trypsin (type XI, 0.5 mg/ml; Sigma). After enzymatic treatment, slices were rinsed and maintained in PIPES buffer at room temperature for ~60 min. Slices were transferred to DMEM buffer (Invitrogen), and the RTN region was identified and excised under a fluorescence-equipped dissecting microscope (Carl Zeiss Discovery V20). The tissue was triturated gently in DMEM buffer using a series of fire-polished Pasteur pipettes (600, 300, and 150 μm, inner diameter), and the DMEM/neuron suspension was placed in a recording chamber on a fixed-stage fluorescence microscope (Carl Zeiss AxioExaminer).

scPCR was performed on dissociated RTN neurons (Lazarenko et al., 2010; Wang et al., 2013). Individual GFP fluorescent cells were aspirated into pipettes containing 10× RT buffer and RNaseOUT (Superscript III; Invitrogen) and expelled (~1 μl) into sterile tubes containing dNTPs, BSA, RNaseOUT, $MgCl_2$, oligo-dT, and random hexamers. The pre-RT mixture was incubated at 65°C, first-strand cDNA synthesis was performed with Superscript III Reverse Transcriptase, and RNA was digested with RNase H and cDNA stored at −20°C. Two rounds of conventional PCR (GoTaq; Promega) used pairs of gene-specific, intron-spanning, outside and nested primer pairs. Primers for Phox2b, GAPDH, VGlut2, TH, and glutamic acid decarboxylase (GAD1) were described previously (Lazarenko et al., 2010; Wang et al., 2013); new primers were prepared for TASK-2 (forward outside, AAGATCCTACAGGTGGTGTCTGAT; reverse outside, GGTTCACACCGGCCACAAAGT; forward nested, CATCACCACCATCGGTTATGGCAA; reverse nested, ACACGTGATCTGAGCCTTCCTCA). Amplicons obtained from each of the primer sets were of the predicted size and were also verified by direct sequencing. We included a no-template negative control for each PCR reaction (H_2O and/or bath solution), and amplification of GAPDH mRNA served as a positive control for each cell.

Data acquisition and analyses. Results are presented as mean ± SEM. Data were analyzed statistically using ANOVA or Student's *t* test, as indicated; *post hoc* pairwise comparisons used the Bonferroni's or Holm–Sidak methods. Differences were considered significant at $p < 0.05$.

Results

TASK-2 deletion blunts or eliminates RTN neuronal pH sensitivity

We tested the hypothesis that alkaline-activated TASK-2 channels contribute to the intrinsic pH sensitivity of RTN chemoreceptor neurons. To this end, we used whole-cell and cell-attached patch recordings to determine effects of changes in bath pH on the firing activity of RTN neurons in brainstem slices derived from global TASK-2 knock-out mice (*TASK-2*$^{-/-}$) and their

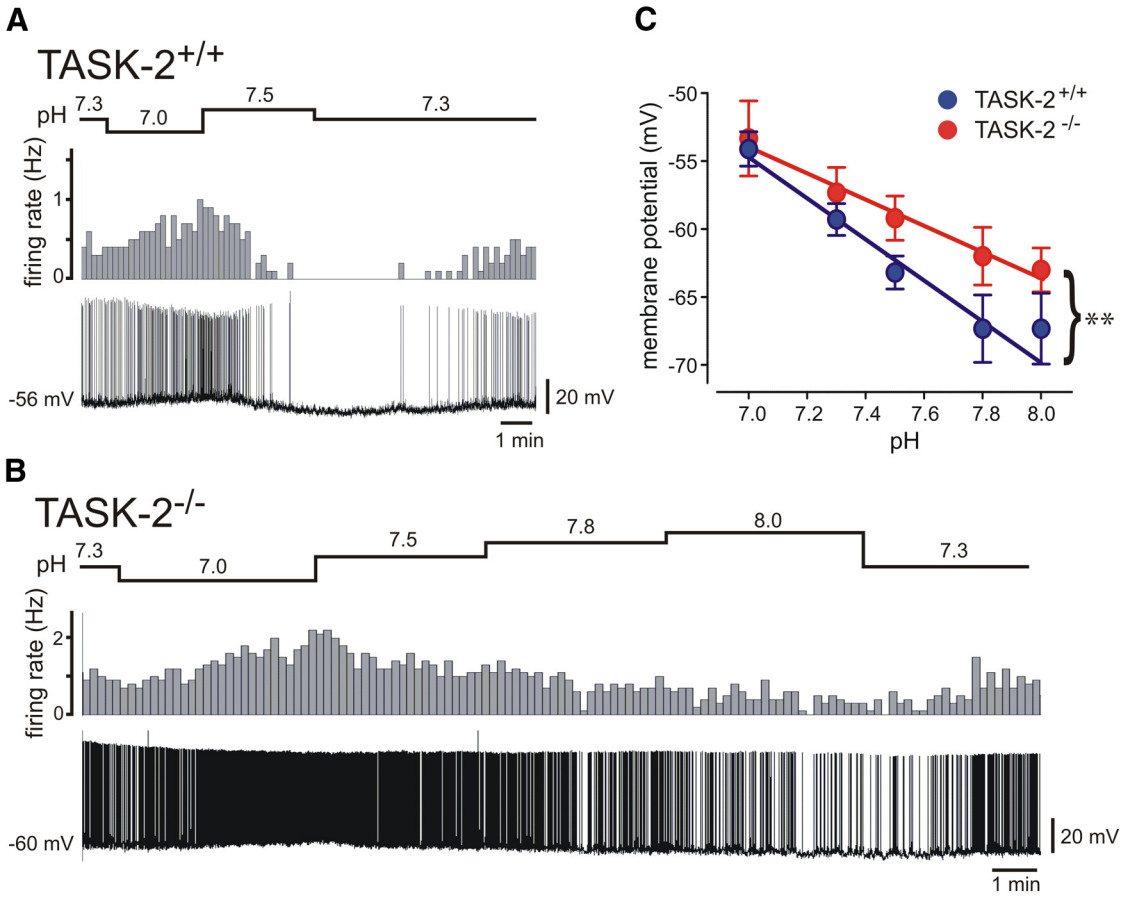

Figure 1. Effects of pH changes on membrane potential and firing rate in RTN neurons from *TASK-2*$^{+/+}$ and *TASK-2*$^{-/-}$ mice. ***A***, ***B***, Representative whole-cell current-clamp recordings of membrane potential (bottom traces) and the associated firing rate (10 s bins; top plots) from GFP-expressing RTN neurons in brainstem slices from *TASK-2*$^{+/+}$ (***A***) and *TASK-2*$^{-/-}$ (***B***) mice during exposure to bath solutions of varying pH. Note that, whereas RTN neurons from both genotypes depolarized and increased firing during acidification (from pH 7.3 to pH 7.0), the effect of alkalization on membrane potential and firing rate was more pronounced at pH 7.5 in the wild-type cell; even with stronger alkalization (to pH 8.0), the *TASK-2*$^{-/-}$ neuron continued to discharge. ***C***, The relationship between membrane potential and bath pH for the subgroup of *TASK-2*$^{+/+}$ and *TASK-2*$^{-/-}$ RTN neurons studied under current-clamp conditions ($n = 10$ and 6); data were fitted by linear regression. There was a genotype-dependent difference in effects of pH on membrane potential ($F_{(2,60)} = 5.6, p < 0.01$).

control littermates (*TASK-2*$^{+/+}$). To identify RTN chemoreceptor neurons independent of their pH sensitivity, we crossed the TASK-2 knock-out mice with a line of BAC transgenic mice in which the Phox2b promoter drives GFP expression in chemosensitive cells of the RTN (Lazarenko et al., 2009; Gestreau et al., 2010).

As depicted for a GFP-expressing RTN neuron from a control *TASK-2*$^{+/+}$ mouse studied under whole-cell current clamp (Fig. 1*A*), bath acidification from pH 7.3 to pH 7.0 caused membrane depolarization with increased spontaneous discharge, whereas alkalization to pH 7.5 hyperpolarized and silenced the neuron; membrane potential and firing rate recovered to baseline levels when the cell was returned to the initial bath solution at pH 7.3. As shown in Figure 1*B*, qualitatively similar responses to changes in pH were also observed in some RTN neurons from *TASK-2*$^{-/-}$ mouse, but the effects appeared blunted, especially during bath alkalization. Thus, whereas this GFP-expressing RTN neuron depolarized and increased firing during acidification to pH 7.0, the discharge slowed only modestly with strong alkalization and the cell maintained its discharge even at pH 8.0. Analysis of averaged effects of pH on membrane potential in RTN neurons from *TASK-2*$^{+/+}$ and *TASK-2*$^{-/-}$ indicated there was a significant genotype-dependent difference, with alkaline-induced hyperpolarization less pronounced in cells deleted for TASK-2 (Fig. 1*C*; $F_{(2,60)} = 5.6, p < 0.01$).

To study a large population of cells under recording conditions that preserve intracellular contents, we used the cell-attached configuration to determine effects of bath pH on the firing activity of RTN neurons in slices from *TASK-2*$^{+/+}$ and *TASK-2*$^{-/-}$ mice (Fig. 2). We found that GFP-expressing RTN neurons from wild-type mice were nearly universally sensitive to changes in pH under these conditions (Fig. 2*A*), as described previously (Lazarenko et al., 2009). However, we found that many cells from *TASK-2*$^{-/-}$ mice showed only modest changes in firing rate as bath pH was altered (Fig. 2*B*) or they did not alter their discharge over a wide range of pH changes (Fig. 2*C*).

To characterize the pH dependence of firing in individual RTN neurons, we calculated the percentage decrease in firing between pH 7.0 and pH 7.8 (Figs. 2*A–C*) and plotted the frequency distribution of those values for cells from *TASK-2*$^{+/+}$ and *TASK-2*$^{-/-}$ mice (Fig. 2*D*). The majority of RTN neurons from *TASK-2*$^{+/+}$ mice showed 100% decrease in firing over this pH range (i.e., they were silenced at pH 7.8). In contrast, the response of cells from *TASK-2*$^{-/-}$ mice was much more variable, with many RTN neurons showing relatively little effect (<30% decrease in firing), some with modest sensitivity (40–90% decrease in firing), and only very few that stopped firing entirely. To provide a consistent criterion for defining whether a cell was pH sensitive, we chose a cutoff value of >30% decrease in firing from pH 7.0 to pH 7.8 (Fig. 2*D*). As shown in Figure 2*E*, this standard

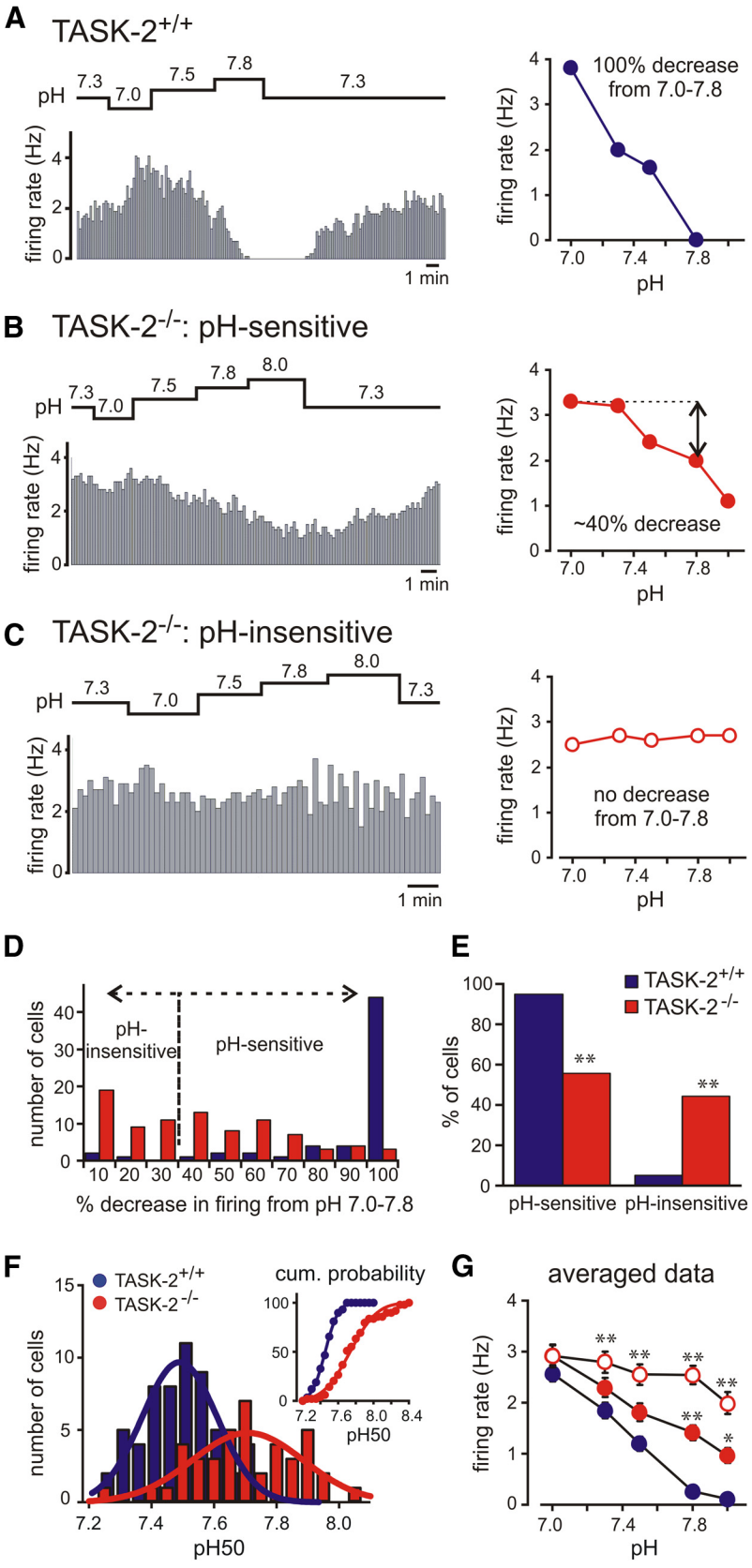

Figure 2. TASK-2 deletion leads to blunted or absent pH sensitivity in RTN neurons. ***A–C***, Representative firing rate responses to changes in bath pH obtained by cell-attached recordings in GFP-expressing RTN neurons from *TASK-2*$^{+/+}$ (***A***) and *TASK-2*$^{-/-}$ (***B***, ***C***) mice. Plots of firing rate at different bath pH levels are provided for each individual neuron (right column). ***D***, Frequency distribution of the percentage decrease in firing from pH 7.0 to pH 7.8 in RTN neurons from *TASK-2*$^{+/+}$ ($n = 61$; blue) and *TASK-2*$^{-/-}$ ($n = 88$; red) mice; a cutoff of >30% decrease in firing was used to classify cells as either pH sensitive or pH insensitive. ***E***, The percentage of cells that were pH sensitive and pH insensitive were significantly different between *TASK-2*$^{+/+}$ and *TASK-2*$^{-/-}$ mice (*$p < 0.0001$ by χ^2 analysis). ***F***, The frequency (and cumulative probability; inset) distributions of pH_{50} values for pH-sensitive RTN neurons from *TASK-2*$^{+/+}$ and *TASK-2*$^{-/-}$ mice; data were fitted with Gaussian distributions that yielded mean pH_{50} values that were significantly different between genotypes (7.45 ± 0.1 vs 7.73 ± 0.2 for *TASK-2*$^{+/+}$ and *TASK-2*$^{-/-}$, $p < 0.0001$). ***G***, The relationship between firing rate and pH for RTN neurons from *TASK-2*$^{+/+}$ mice and for the subpopulations of RTN neurons from *TASK-2*$^{-/-}$ mice that were classified as pH sensitive and pH insensitive. *$p < 0.05$ and **$p < 0.01$ versus *TASK-2*$^{+/+}$ by two-way ANOVA.

defined nearly all RTN neurons from *TASK-2*$^{+/+}$ mice as pH sensitive (95%, $n = 58$ of 61), whereas only 56% of RTN neurons from *TASK-2*$^{-/-}$ mice were characterized as pH sensitive by this criterion ($n = 49$ of 88).

To provide a quantitative measure of the effects of TASK-2 deletion on firing responses to alkalization among the pH-sensitive populations of RTN neurons from *TASK-2*$^{+/+}$ and *TASK-2*$^{-/-}$ mice, we calculated a pH_{50} value for each cell (i.e., the pH at which firing frequency was reduced to half that observed at pH 7.0). As depicted in Figure 2*F*, we obtained a continuous distribution of pH_{50} values from both groups that could be well fitted by Gaussian functions. It is worth noting that we could not discern the bimodal distribution in pH_{50} values from wild-type cells characteristic of type I and type II cells we described previously (i.e., with pH_{50} values of ~7.3 and ~7.6; Lazarenko et al., 2009). Instead, this sample of *TASK-2*$^{+/+}$ RTN neurons was characterized by a single broad peak, with an intermediate mean pH_{50} value (7.45 ± 0.01). Importantly, the pH-sensitive RTN neurons from *TASK-2*$^{-/-}$ mice were defined by a significantly higher mean pH_{50} value (7.74 ± 0.01, $p < 0.0001$), indicating that deletion of TASK-2 led to a blunted response to alkalization (i.e., firing was reduced only at higher pH levels in those neurons).

The diminished pH sensitivity in RTN neurons after TASK-2 deletion was also apparent in plots of the averaged relationship between firing rate and bath pH in the different cell populations (Fig. 2*G*). That is, compared with the response from *TASK-2*$^{+/+}$ cells, the effect of alkalization on firing in pH-sensitive *TASK-2*$^{-/-}$ RTN neurons was significantly dampened. The additional subset of pH-insensitive cells from *TASK-2*$^{-/-}$ mice showed virtually no change in firing through the range

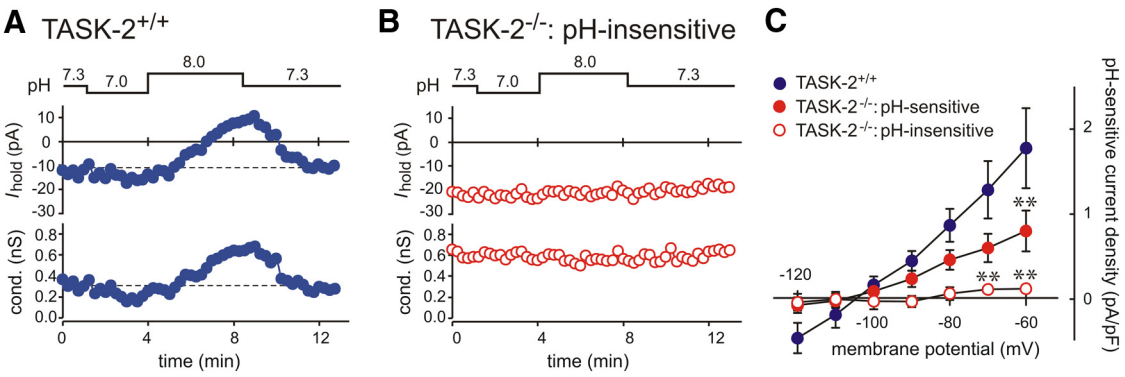

Figure 3. Alkaline-activated background K^+ current is diminished or absent in *TASK-2*$^{-/-}$ RTN neurons. Voltage-clamp recordings were obtained from GFP-expressing RTN neurons during bath acidification and alkalization; before gaining whole-cell access, each cell was first characterized as pH sensitive or pH insensitive based on firing responses to pH changes in the cell-attached configuration (Fig. 2). ***A***, In a pH-sensitive *TASK-2*$^{+/+}$ RTN neuron, acidification decreased holding current (top trace) and conductance (bottom trace) and alkalization caused a reversible outward shift in current with an increase in conductance. ***B***, In a pH-insensitive *TASK-2*$^{-/-}$ RTN neuron, changes in bath pH had little effect on holding current or conductance. ***C***, Averaged *I–V* relationship of the pH-sensitive current density (pH 8.0 minus pH 7.0) for RTN neurons from *TASK-2*$^{+/+}$ mice ($n = 13$) and for RTN neurons from *TASK-2*$^{-/-}$ mice that were classified as pH sensitive ($n = 12$) and pH insensitive ($n = 7$). Note that the weakly rectifying alkaline-activated K^+ current seen in *TASK-2*$^{+/+}$ neurons was reduced in pH-sensitive RTN neurons from *TASK-2*$^{-/-}$ mice and absent in pH-insensitive *TASK-2*$^{-/-}$ RTN neurons. $^{**}p < 0.01$ versus *TASK-2*$^{+/+}$ by two-way ANOVA.

from pH 7.0 to pH 7.8, with a slightly sharper decrease in discharge evident only at pH 8.0. Note that the averaged firing rate was not different among any of these groups at pH 7.0, but the relationships diverged at higher pH values at which alkaline-activated TASK-2 channels are most active. Because nearly equal populations of RTN neurons were defined as pH sensitive or pH insensitive in *TASK-2*$^{-/-}$ mice (Fig. 2*E*), the aggregate firing response from the entire population of TASK-2-deleted RTN neurons falls approximately midway between those two firing versus pH curves (data not shown) and is significantly higher than that for *TASK-2*$^{+/+}$ cells ($p < 0.0001$ by two-way ANOVA). At pH 7.3, the combined average firing rate for pH-sensitive and pH-insensitive *TASK-2*$^{-/-}$ RTN neurons was greater than that for *TASK-2*$^{+/+}$ cells (2.6 ± 0.1 vs 1.9 ± 0.2 Hz, $p < 0.01$), and this difference was further enhanced at more alkalized pH levels.

Together, these data indicate that pH sensitivity is generally diminished across all RTN neurons from TASK-2 knock-out mice and that TASK-2 channels are required for pH sensitivity in ~44% of those cells.

A pH-sensitive background K^+ current is reduced in amplitude or absent in RTN neurons from *TASK-2*$^{-/-}$ mice

We previously described a pH-sensitive background K^+ current in RTN neurons with characteristics not unlike those of the alkaline-activated TASK-2 channel (Mulkey et al., 2004, 2007; Lazarenko et al., 2010). Thus, after assessing the pH sensitivity in GFP-expressing RTN neurons from *TASK-2*$^{+/+}$ ($n = 12$) and *TASK-2*$^{-/-}$ ($n = 19$) mice in the cell-attached configuration, we obtained whole-cell access and used voltage-clamp recordings to examine pH-sensitive currents in those cells (Fig. 3). As shown in Figure 3*A* for a cell from a *TASK-2*$^{+/+}$ mouse, acidification of the bath solution (from pH 7.3 to pH 7.0) caused an inward shift in holding current at −60 mV that was accompanied by a decrease in conductance, whereas bath alkalization (from pH 7.0 to pH 8.0) resulted in an outward shift in holding current with an increase in conductance. We obtained qualitatively similar results from the subgroup of RTN neurons from *TASK-2*$^{-/-}$ mice that showed firing responses that were characterized as pH sensitive (data not shown). However, in the pH-insensitive population of RTN neurons obtained from *TASK-2*$^{-/-}$ mice ($n = 7$), there was little effect of bath alkalization on holding current or conductance, as exemplified in the cell of Figure 3*B*.

We determined *I–V* relationships for the pH-sensitive current in each of these groups of RTN neurons, obtained by digital subtraction of currents in pH 7.0 from those in pH 8.0 (and normalized to cell capacitance, i.e., current density). In *TASK-2*$^{+/+}$ cells, the averaged alkaline-activated current was weakly rectifying, with a reversal potential near the predicted value for E_K (approximately −95 mV); this is typical of the pH-sensitive background K^+ current reported previously for wild-type RTN neurons. In the pH-sensitive RTN neurons from *TASK-2*$^{-/-}$ mice, the *I–V* was similar in shape to that of *TASK-2*$^{+/+}$ cells but diminished in amplitude. In contrast, there was essentially no alkaline-activated current in those pH-insensitive *TASK-2*$^{-/-}$ neurons that failed to alter their discharge in response to changes in bath pH. These data suggest that TASK-2 channels are required for the alkaline-activated background K^+ current in the subset of pH-insensitive RTN neurons; in the other RTN neurons from *TASK-2*$^{-/-}$ mice, although TASK-2 channels contribute to the overall background K^+ current, currents from other background K^+ channels contribute to pH sensitivity.

Most chemosensitive RTN neurons express TASK-2, with approximately half the population expressing higher levels

The data presented to this point suggest a prominent, even necessary, role for TASK-2 channels in the pH sensitivity of nearly half the population of Phox2b (and GFP)-expressing RTN neurons and a more modest but still measurable contribution in the other half of those cells. In light of these results, we sought to examine whether there is a differential distribution of TASK-2 expression in RTN neurons.

There are no well established TASK-2 antibodies available for immunohistochemistry. Therefore, we used X-gal staining as a surrogate for TASK-2 expression in RTN neurons, taking advantage of the β-galactosidase cassette that was integrated into the TASK-2 locus by the gene trap construct in this knock-out mouse line (Leighton et al., 2001; Gestreau et al., 2010); as expected, X-gal staining was not observed in tissue from *TASK-2*$^{+/+}$*–Jx* mice (data not shown). The Phox2b-expressing chemosensitive population of RTN neurons was defined in these mice by immunohistochemical detection of GFP expression from the Phox2b BAC transgene, absence of staining for TH, and by their anatomical localization (Stornetta et al., 2006; Lazarenko et al., 2009). As shown in Figure 4*A*, we detected overlapping expression of GFP

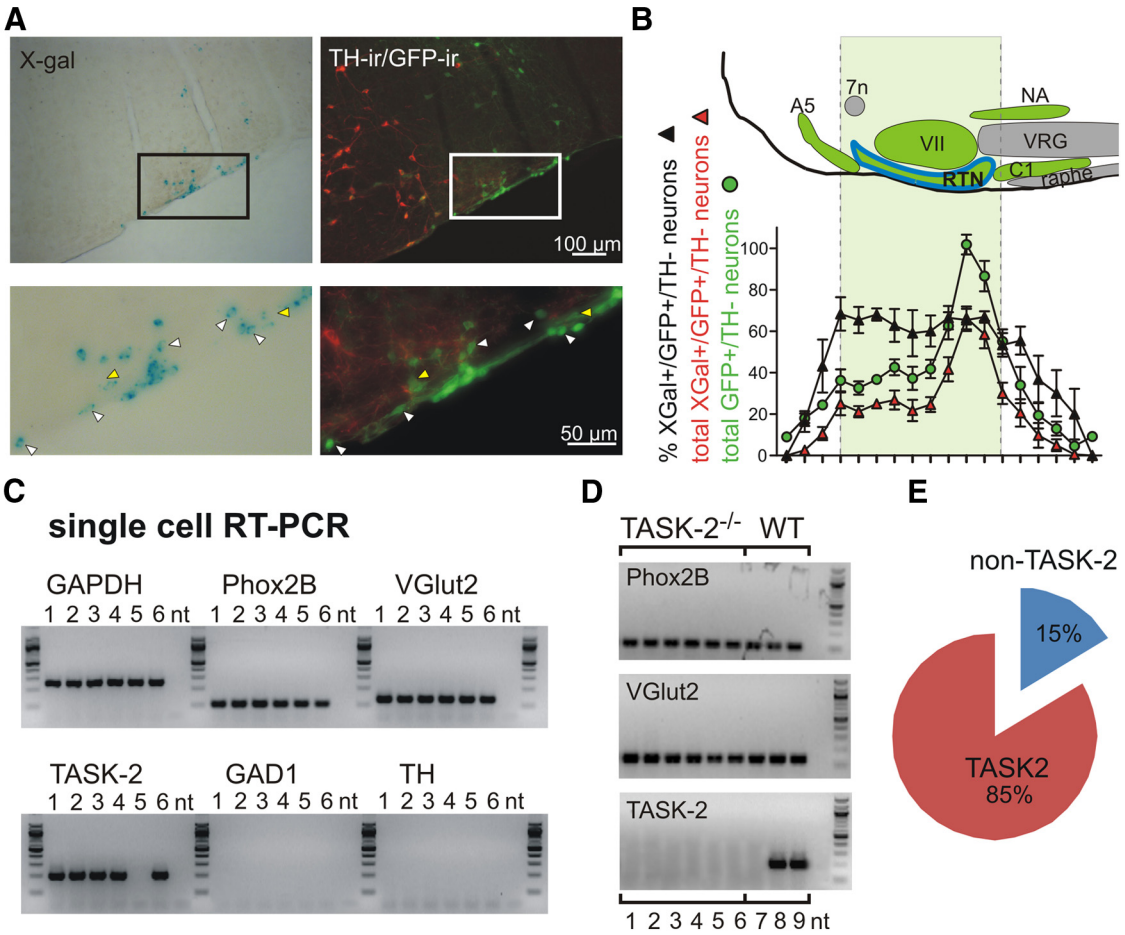

Figure 4. TASK-2 is strongly expressed in a subset of Phox2b-expressing RTN neurons. ***A***, Photomicrographs of histochemical staining for X-gal (left) and GFP and TH (right) in the RTN region of the rostroventrolateral medulla. The boxed region depicted in the lower-magnification image (top) is shown at greater magnification (bottom). Note that, among the double-positive neurons (GFP^+/X-gal^+; white arrowheads), there were also some GFP^+ neurons in the RTN that were not stained with X-gal (yellow arrowheads). ***B***, Top, Schematic of the brainstem region containing the RTN, delimiting the landmarks used to align sections for cell counts. Bottom, Quantification of the total number of Phox2b-expressing chemoreceptor neurons in each section (defined as GFP^+/TH^-) and of the percentage of those RTN neurons that also showed detectable X-gal staining. Overall, β-galactosidase expression was observed in ~63% (321 ± 40 of 504 ± 25 RTN neurons) of these RTN neurons, with an even fractional distribution throughout the rostrocaudal extent of the nucleus. 7n, Facial nerve; VII, facial nucleus; VRG, ventral respiratory group; NA, nucleus ambiguus. ***C***, scPCR from a representative sample of GFP-expressing dissociated RTN neurons (lanes 1–6) revealed expression of Phox2b and VGlut2 in all cells tested, with no evidence for GAD1 and TH, as expected for chemosensitive RTN neurons. Notably, we detected TASK-2 in all but one of those RTN neurons (lane 5). The positive control GAPDH transcript was universally detectable, and no-template negative controls were included in all reactions (nt, lane 7). ***D***, Verification by scPCR of TASK-2 deletion from individual Phox2b- and VGlut2-expressing RTN neurons obtained from *TASK-2*$^{-/-}$ mice (lanes 1–6); TASK-2 expression was evident in two of three wild-type RTN neurons processed concurrently. ***E***, Quantification of scPCR data revealed TASK-2 expression in 85% of RTN neurons ($n = 52/61$).

and X-gal in the RTN region of the rostral ventrolateral medulla. At higher power, it was clear that nearly all X-gal-stained cells in the RTN were GFP immunoreactive (GFP^+, ~98%). However, we found a number of GFP-expressing cells that showed no detectable X-gal staining (yellow arrowheads). We quantified the total number of GFP^+/TH^- neurons in sections encompassing the entire rostrocaudal extent of the RTN in young mice (P11–P24, $n = 5$) and then determined the percentage of those neurons that also showed X-gal staining (Fig. 4*B*). The distribution and number of GFP-labeled cells we observed was similar to that described previously for GFP (and Phox2b) expression in the Jx99 line of mice (Lazarenko et al., 2009), indicating that deletion of TASK-2 did not affect specification or maintenance of this population of neurons. Over the entire nucleus, we found that 63 ± 5.4% of GFP^+/TH^- neurons showed clearly detectable X-gal staining, suggesting that TASK-2 is expressed most prominently in this group of cells.

As mentioned, X-gal staining is a surrogate for TASK-2 expression; it assumes that expression of β-galactosidase from the gene trap is comparable with that of the endogenous TASK-2 gene from the native locus (Leighton et al., 2001; Gestreau et al., 2010). To provide a sensitive and direct assay of TASK-2 expression in RTN neurons, we used a nested, multiplex scPCR reaction to amplify TASK-2 transcripts from acutely dissociated GFP fluorescent neurons (Lazarenko et al., 2010; Wang et al., 2013); we simultaneously confirmed the presence of two markers of chemosensitive RTN neurons, Phox2b and VGlut2, and absence of markers for GABAergic (GAD1) and catecholaminergic (TH) neurons (Stornetta et al., 2006; Wang et al., 2013). The experiment shown in Figure 4*C* reveals TASK-2 amplicons in five of six individual Phox2b-expressing, glutamatergic RTN neurons. In control experiments, we verified deletion of TASK-2 in RTN neurons from knock-out mice (Fig. 4*D*, lanes 1–6); in this particular experiment, TASK-2 was simultaneously detected in two of three RTN neurons from wild-type mice (Fig. 4*D*, lanes 7–9). Overall, we detected TASK-2 expression in 85% of the RTN neurons tested by scPCR ($n = 52$ of 61; Fig. 4*E*), a greater fraction than obtained by using X-gal staining. Together, these data suggest

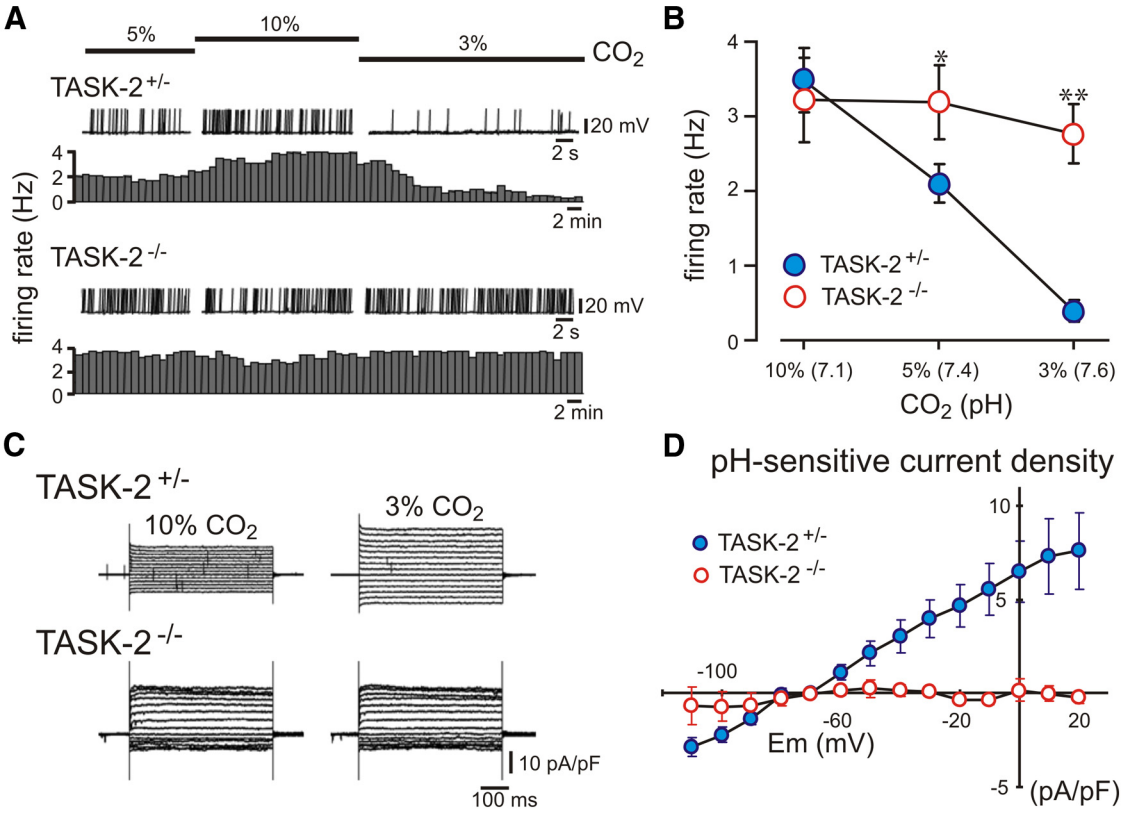

Figure 5. TASK-2 deletion ablates pH sensitivity in all RTN neurons selected for β-galactosidase activity. ***A***, Representative whole-cell current-clamp recordings of membrane potential (top plots) and the associated firing rate (bottom traces) from RTN neurons stained with FDG, a fluorogenic β-galactosidase substrate, in slices from heterozygous *TASK-2*$^{+/-}$ and homozygous *TASK-2*$^{-/-}$ mice during exposure to bath solutions equilibrated with different levels of CO_2 (3, 5, and 10%, corresponding to pH 7.6, pH 7.4, and pH 7.1). The *TASK-2*$^{+/-}$ cell showed typical pH-dependent changes in membrane potential and firing rate, whereas the *TASK-2*$^{-/-}$ RTN neuron was insensitive to both acidification and alkalization. All FDG-labeled *TASK-2*$^{-/-}$ neurons failed to respond to changes in pH. ***B***, The relationship between firing rate and CO_2 (pH) for FDG-fluorescent RTN neurons from *TASK-2*$^{+/-}$ ($n = 14$) and *TASK-2*$^{-/-}$ ($n = 11$) mice. *$p < 0.05$, **$p < 0.0001$ versus *TASK-2*$^{+/-}$. ***C***, Using whole-cell voltage clamp under conditions that block most voltage-dependent K^+ channels (tetraethylammonium, 10 mM; 4-AP, 3 mM; and barium, 10 μM), currents were evoked with a series of voltage steps in an acidified (left, 10% CO_2, pH 7.1) and alkalized bath (right, 3% CO_2, pH 7.6) in FDG-labeled RTN neurons from *TASK-2*$^{+/-}$ (top) and *TASK-2*$^{-/-}$ (bottom) mice. ***D***, Averaged *I–V* relationship of pH-sensitive current density (10% CO_2 minus 3% CO_2) for RTN neurons from *TASK-2*$^{+/-}$ ($n = 10$) and *TASK-2*$^{-/-}$ ($n = 5$) mice. Note that the alkaline-activated K^+ current seen in *TASK-2*$^{+/-}$ neurons was totally absent in FDG-fluorescent *TASK-2*$^{-/-}$ RTN neurons.

that TASK-2 expression can be detected in the majority of RTN neurons but that levels of TASK-2 expression may be higher in the subgroup of cells that are recognized by detectable β-galactosidase activity from the TASK-2 locus in this knock-out mouse line.

TASK-2 channels are required for pH sensitivity in those RTN neurons with high levels of TASK-2 expression

To this point, our data indicate that a subgroup of GFP-expressing RTN neurons we tested require TASK-2 expression for their pH sensitivity (~44%), and a comparable population showed detectable expression of β-galactosidase from the TASK-2 locus (~63%). This suggested the possibility that measurable β-galactosidase activity might identify the specific subpopulation of RTN neurons for which TASK-2 expression is critical for pH sensitivity.

To test this possibility, we developed a method to identify and target this population of RTN neurons for electrophysiological recordings by incubating brainstem slices with FDG, a fluorogenic β-galactosidase substrate. Because this method required at least one copy of the gene trap construct, we used heterozygous *TASK-2*$^{+/-}$ littermates (rather than *TASK-2*$^{+/+}$ mice) as controls for homozygous *TASK-2*$^{-/-}$ mice in these experiments. As shown in Figure 5*A*, we found that RTN neurons from heterozygous *TASK-2*$^{+/-}$ mice ($n = 14$) responded to changes in pH induced by varying CO_2 levels in a HCO_3^--containing buffer in a manner essentially identical to that described for *TASK-2*$^{+/+}$ mice when pH was changed by altering fixed acid in HEPES-based bath solution (Figs. 1, 2); that is, cells depolarized and increased firing during bath acidification, and they hyperpolarized and decreased firing during bath alkalization. However, in these experiments in which cells were targeted based on β-galactosidase expression, we found that RTN neurons from *TASK-2*$^{-/-}$ mice were uniformly insensitive to bath pH ($n = 11$). Indeed, as shown in the averaged data of Figure 5*B*, FDG-labeled *TASK-2*$^{-/-}$ cells maintained their discharge throughout the pH range, in contrast to the typical pH-dependent decrease in RTN neuronal firing that was observed in cells from *TASK-2*$^{+/-}$ mice. Notably, the resting membrane potential at pH 7.4 for FDG-labeled RTN neurons from *TASK-2*$^{-/-}$ mice was depolarized compared with that of the *TASK-2*$^{+/-}$ cells (-52.9 ± 1.4 vs -65.1 ± 1.5 mV, $p < 0.0001$), as expected for deletion of a background K^+ channel and corresponding to the higher basal firing rate of these neurons at physiological pH. We found no evidence for a population of pH-sensitive RTN neurons from *TASK-2*$^{-/-}$ mice when cells were selected based on β-galactosidase activity. These data suggest that TASK-2 contributes to stabilizing the resting membrane potential in this subpopulation of RTN neurons that express easily detectable β-galactosidase activity (and presumably higher levels of TASK-2) and that these cells are

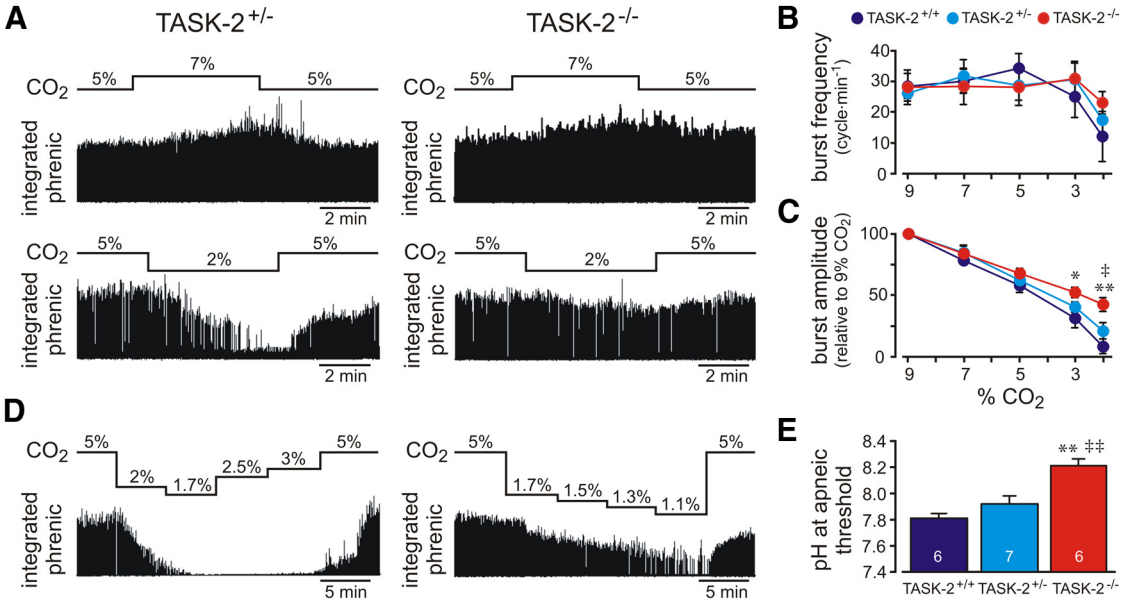

Figure 6. TASK-2 deletion blunts effects of alkalization on respiratory-like neural output in an *in situ* preparation. ***A***, A working heart–brainstem preparation was used to examine effects of respiratory acidosis (7% CO_2; top traces) and respiratory alkalosis (2% CO_2; bottom traces) on integrated phrenic nerve activity in *TASK-2*$^{+/-}$ (left) and *TASK-2*$^{-/-}$ (right) mice. Phrenic nerve amplitude was reversibly increased in 7% CO_2 and decreased in 2% CO_2, but the inhibition by 2% CO_2 was less pronounced in *TASK-2*$^{-/-}$ mice. ***B***, For both genotypes, respiratory frequency was unaffected by changes in CO_2 from 3 to 9%; frequency decreased significantly only when CO_2 was reduced to ≤2%. ***C***, Effects on phrenic nerve amplitude of raising CO_2 (from 5 to 7 or 9%) were not different between *TASK-2*$^{+/-}$ mice and *TASK-2*$^{-/-}$ mice; however, decreases in phrenic nerve amplitude associated with lowering CO_2 (to 3 and 2%) were relatively blunted in *TASK-2*$^{-/-}$ mice. $^{*}p < 0.05$, $^{**}p < 0.001$ versus *TASK-2*$^{+/+}$; $^{‡}p < 0.05$ versus *TASK-2*$^{+/-}$ by two-way ANOVA. ***D***, Apneic threshold (i.e., the pH when phrenic nerve activity was eliminated) was determined by sequentially lowering CO_2 levels in preparations from *TASK-2*$^{+/-}$ (left) and *TASK-2*$^{-/-}$ (right) mice. Note the more modest effect of respiratory alkalosis on phrenic nerve discharge in the *TASK-2*$^{-/-}$ exemplar. ***E***, Averaged values of pH at apneic threshold were significantly higher in preparations from *TASK-2*$^{-/-}$ mice. $^{**}p < 0.001$ versus *TASK-2*$^{+/+}$; $^{‡‡}p < 0.01$ versus *TASK-2*$^{+/-}$ by one-way ANOVA with sample size indicated.

strictly dependent on TASK-2 channels for their pH sensitivity. Consistent with this, whereas β-galactosidase-expressing *TASK-2*$^{+/-}$ neurons showed a robust pH-sensitive and voltage-independent K^+ current, this current was not seen at all in FDG-labeled RTN neurons from *TASK-2*$^{-/-}$ mice (Fig. 5*C*,*D*). Thus, *TASK-2*$^{-/-}$ RTN neurons selected based on β-galactosidase activity appear to be functionally equivalent to the pH-insensitive subset of Phox2b-expressing *TASK-2*$^{-/-}$ cells that appear to depend critically on TASK-2 for their pH sensitivity.

The respiratory chemoreflex is blunted in a working heart–brainstem preparation from *TASK-2*$^{-/-}$ mice

Our data indicate that RTN neurons from *TASK-2*$^{-/-}$ mice show a blunted response to alkaline pH, i.e., firing rate is approximately equal to that of cells from *TASK-2*$^{+/+}$ mice at relatively acidified pH levels but better maintained at more alkalized pH levels (Fig. 2*F*). To test for respiratory chemosensitivity in a more intact preparation over a wide range of pH/CO_2, we used the working heart–brainstem preparation. In this *in situ* preparation, CO_2 and bicarbonate levels in the brainstem perfusate are controlled and phrenic nerve activity serves as a measure of central respiratory outflow. As reported previously (Abdala et al., 2009; Marina et al., 2010), we found that respiratory acidosis evoked by increasing inspired CO_2 from 5 to 7 or 9% caused an increase in phrenic burst amplitude with little effect on phrenic burst frequency (Fig. 6*A*–*C*). The acidosis-induced increase in phrenic burst amplitude was similar in preparations from *TASK-2*$^{+/+}$, *TASK-2*$^{+/-}$, and *TASK-2*$^{-/-}$ littermates (Fig. 6*C*). Conversely, respiratory alkalosis obtained by decreasing CO_2 from 5 to 3 or 2% caused a decrease in phrenic burst amplitude. The alkalosis-induced decrease in phrenic burst amplitude was blunted in preparations from *TASK-2*$^{-/-}$ mice compared with TASK-2-expressing littermates (Fig. 6*A*, *C*), with a significantly smaller effect evident at 3% CO_2 (52.4 ± 4.2% for *TASK-2*$^{-/-}$ vs 31.6 ± 7.6% for *TASK-2*$^{+/+}$) and at 2% CO_2 (42.6 ± 5.5% for *TASK-2*$^{-/-}$ vs 21.2 ± 6.6% for *TASK-2*$^{+/-}$ and 8.7 ± 5.8% for *TASK-2*$^{+/+}$). An additional decrease in phrenic burst frequency was observed at 2% CO_2, but this was not significantly different between genotypes (Fig. 6*B*).

In a subset of experiments (Fig. 6*D*), we progressively lowered CO_2 levels to determine the effect of TASK-2 deletion on the apneic threshold (i.e., the pH of the perfusate at which respiratory outflow was eliminated). Note that the apneic threshold occurs at more alkalized levels *in situ* compared with *in vivo* preparations (Takakura et al., 2008; Molkov et al., 2011), and, in some *in situ* preparations from *TASK-2*$^{-/-}$ mice, we did not observe a cessation of phrenic activity even at the lowest CO_2 levels tested (Fig. 6*D*); for those cases, we reported the lowest pH value measured as the apneic threshold. As shown in Figure 6*E*, the pH at apneic threshold was significantly higher in preparations from *TASK-2*$^{-/-}$ (pH 8.2 ± 0.05, $n = 6$) compared with *TASK-2*$^{+/-}$ littermate controls (pH 7.9 ± 0.05, $n = 7$, $p < 0.01$) and *TASK-2*$^{+/+}$ mice (pH 7.8 ± 0.04, $n = 6$, $p < 0.001$). Thus, deletion of alkaline-activated TASK-2 channel is associated with diminished respiratory responses to hypocapnic alkalosis *in situ*.

Discussion

Phox2b-expressing, glutamatergic neurons of the RTN are central respiratory chemosensors, i.e., they provide a CO_2-dependent excitatory drive to brainstem respiratory networks. The pH sensitivity of these neurons is, at least in part, an intrinsic property (Wang et al., 2013), but the molecular basis for pH sensing has not been defined (Guyenet et al., 2010; Feldman et al., 2013). In this paper, we used a knock-out mouse model to dem-

onstrate that TASK-2, an alkaline-activated K2P channel with a highly restricted brainstem expression, including in Phox2b-expressing RTN neurons (Gestreau et al., 2010), contributes to the pH-sensitive background K^+ current observed previously in those chemosensitive RTN neurons (Mulkey et al., 2004, 2007). Moreover, we used a working heart–brainstem preparation to show that ablation of TASK-2 attenuated the inhibition of respiratory output typically evoked by hypocapnic alkalosis and raised the pH level at which the central drive to breathe is eliminated (i.e., the apneic threshold). Thus, this work identifies the TASK-2 channel as a molecular substrate for intrinsic pH sensitivity within this defined population of central respiratory chemoreceptor neurons. The residual CO_2/H^+-dependent responses of RTN neurons and of the respiratory network in TASK-2 knock-out mice imply that alternative/compensatory cellular and molecular mechanisms are also engaged in respiratory chemosensitivity, at least under conditions when TASK-2-mediated RTN neuronal chemosensitivity is disrupted.

TASK-2 and other pH-sensitive background K^+ channels in RTN neurons

We found that deletion of TASK-2 led to complete disruption of pH-dependent firing activity and elimination of the attendant alkalosis-activated K^+ current in ~44% of the Phox2b-expressing neurons within the RTN. Correspondingly, we detected β-galactosidase enzyme activity, a surrogate of TASK-2 expression in knock-out mice (Leighton et al., 2001), in a comparable fraction of RTN cells (~63%). Moreover, we found that an FDG-labeled subpopulation of RTN neurons was entirely pH insensitive *in vitro*. We assume that the higher β-galactosidase activity in that group of neurons is indicative of greater expression from the TASK-2 locus, likely accounting for our observation that those particular RTN neurons appear to rely exclusively on TASK-2 for their pH sensitivity. Of note, TASK-2 expression could be detected in a larger percentage of cells (~85%) by using the more sensitive scPCR technique. Accordingly, the pH-dependence of firing activity was depressed and the alkalosis-activated background K^+ current amplitude was reduced across all *TASK-2*$^{-/-}$ RTN neurons. This was true even among those cells that continued to meet our criterion for pH sensitivity. Thus, in neonatal mice, TASK-2 channels are fully responsible for chemosensitivity in the specific group of RTN neurons that appear to have the highest levels of TASK-2 gene expression, but those channels also provide a clear contribution to pH sensitivity in the majority of RTN neurons.

We found a residual pH-sensitive background K^+ current in the subset of TASK-2-deleted RTN neurons that retained some responsiveness to changes in pH. This suggests that a molecularly distinct, although functionally similar, background K^+ channel may also contribute to pH sensitivity in this subgroup of RTN neurons. We suggest that it may serve to augment pH-dependent responses in the subgroup of cells that express lower levels of TASK-2. Thus, there may be redundant pH-sensing mechanisms within the Phox2b-expressing RTN chemosensory neuronal cell group. At this point, however, we cannot rule out the possibility that this reflects a compensatory pH-sensitive K^+ current that only becomes prominent in RTN neurons from *TASK-2*$^{-/-}$ mice.

Effects of TASK-2 deletion on RTN electrophysiological properties are most prominent at alkalized pH

Despite its similar moniker, TASK-2 is not grouped among the acid-sensitive K2P channels TASK-1 and TASK-3, but instead is more closely aligned with the alkaline-activated K2P subgroup, along with TALK-1 (K2P16) and TALK-2 (K2P17) (Lesage and Barhanin, 2011). The p*K*a for TASK-2 is at pH ~7.6–7.8; its activity is low near physiological pH and increases sharply with alkalization (Lesage and Barhanin, 2011). These pH-dependent channel properties were reflected in the functional consequences of TASK-2 deletion. Indeed, as expected from elimination of the membrane hyperpolarizing influence of TASK-2, which would increase with greater alkalization, the genotype-dependent differences in membrane potential and firing rate were increasingly enhanced throughout the alkalized range. Thus, we saw no significant difference in membrane potential or firing rate between TASK-2-expressing and TASK-2-deleted RTN neurons at acidified levels (i.e., at pH 7). However, at alkalized levels at which wild-type RTN neurons are typically silenced (pH 7.6–7.8), action potential discharge persisted in the pH-sensitive *TASK-2*$^{-/-}$ RTN neurons and was fully retained in the pH-insensitive group of those cells.

Effects of TASK-2 deletion on central respiratory output are apparent during respiratory alkalosis near apneic threshold

Using an *in situ* working heart–brainstem preparation, we found that integrated central respiratory output was better maintained during hypocapnic alkalosis in preparations from *TASK-2*$^{-/-}$ mice compared with those from TASK-2-expressing mice; there were no differences in respiratory output between genotypes during hypercapnic acidosis. Thus, these *in situ* experiments are generally consistent with our cellular data in supporting the idea that elevated TASK-2 background K^+ channel activity during alkalization, and the concomitant inhibition of RTN neurons, serves to reduce respiratory output during hypocapnic alkalosis. The preserved phrenic nerve response to hypercapnic acidosis we observed *in situ* from *TASK-2*$^{-/-}$ preparations could reflect the diminished role for TASK-2 in modulating aggregate RTN firing activity at those pH levels, as documented in our cellular recordings. Alternatively, contributions from other peripheral and/or central chemosensor cell types could become more prominent at raised CO_2 levels (Putnam et al., 2004; Nattie and Li, 2006; Guyenet et al., 2010; Corcoran et al., 2013; Feldman et al., 2013). A greater contribution from peripheral chemoreceptors (carotid bodies) in this preparation might explain why TASK-2 deletion reduced pH modulation of individual RTN neurons more than the overall respiratory chemoreflex.

Although these basic conclusions regarding a role for TASK-2 in RTN chemoreceptor neurons and central respiratory chemosensitivity are generally valid across preparations of increasing complexity, there are some apparent inconsistencies that bear mentioning. For example, although aggregate RTN neuronal firing levels were higher in *TASK-2*$^{-/-}$ mice at normal physiological pH in brainstem slices *in vitro*, there were no differences in baseline respiratory output *in situ* (Fig. 2*G* at pH 7.4 vs Fig. 6*D* at 5% CO_2) or ventilatory activity *in vivo* before CO_2 challenge (0% CO_2; see plethysmography data by Gestreau et al., 2010, their Fig. 3*B*). Comparing the *in vitro* to the more intact preparations, we must also emphasize that RTN neuronal responses were obtained in slices prepared from neonatal mice, whereas *in situ* and *in vivo* experiments were performed in more mature animals; developmental changes in central respiratory chemosensitivity are well described (Stunden et al., 2001; Davis et al., 2006; Nattie and Li, 2006). Moreover, although selective ablation of RTN chemosensitive neurons eliminates respiratory chemosensitivity at birth, a partial CO_2-evoked ventilatory response recovers after a few weeks that likely reflects compensatory development of an alter-

native chemosensory mechanism (Ramanantsoa et al., 2011). A similar alternative mechanism could develop in the face of diminished RTN neuronal chemosensitivity resulting from TASK-2 deletion and influence integrated respiratory chemoresponses measured *in situ* or *in vivo*. It is also worth noting that metabolic acidosis is known to occur in TASK-2 knock-out mice (Warth et al., 2004), and it is possible that long-term acidosis could lead to compensatory changes in respiratory chemosensitivity measured *in situ* or *in vivo*. We found that CO_2-induced acidification had identical effects on phrenic output in TASK-2-expressing and TASK-2-deleted mice *in situ*, in which acute metabolic acidosis was eliminated, whereas hypercapnic acidosis evoked a blunted effect on breathing in *TASK-2*$^{-/-}$ mice studied previously *in vivo*, in which continued metabolic acidosis could affect respiratory responses (Gestreau et al., 2010). Finally, the *in situ* preparation used here allowed examination of the effects of low CO_2 at alkalized pH levels in which effects of TASK-2 deletion on neuronal firing were most prominent; this was not done previously in experiments with conscious *TASK-2*$^{-/-}$ mice *in vivo*, which only examined effects of raised CO_2 and acidosis on breathing (Gestreau et al., 2010).

In conclusion, this work establishes a contribution of TASK-2 channels to the pH sensitivity of the majority of Phox2b-expressing RTN neurons. In nearly half of these RTN cells, notably those with elevated TASK-2 gene expression, the channel appears to fully account for the pH-sensitive background K^+ current and pH-dependent effects on neuronal firing. In the other RTN neurons, a blunted pH sensitivity is observed that may be attributable to a redundant or compensatory pH-sensitive background K^+ current. The loss of TASK-2 was associated with less pronounced inhibition of respiratory output during respiratory alkalosis and a higher pH threshold for breathing cessation, consistent with elevated RTN neuronal firing at high pH in *TASK-2*$^{-/-}$ mice. Given the remarkably discrete localization of TASK-2 within the CNS (Gestreau et al., 2010) and its contribution to RTN neuronal firing and respiratory output, we suggest that selective inhibition of TASK-2 to shift the CO_2 response curve and bias the respiratory system away from apnea might provide a new avenue to support breathing.

References

Abbott SB, Stornetta RL, Fortuna MG, Depuy SD, West GH, Harris TE, Guyenet PG (2009) Photostimulation of retrotrapezoid nucleus Phox2b-expressing neurons *in vivo* produces long-lasting activation of breathing in rats. J Neurosci 29:5806–5819. CrossRef Medline

Abbott SB, Stornetta RL, Coates MB, Guyenet PG (2011) Phox2b-expressing neurons of the parafacial region regulate breathing rate, inspiration, and expiration in conscious rats. J Neurosci 31:16410–16422. CrossRef Medline

Abdala AP, Rybak IA, Smith JC, Paton JF (2009) Abdominal expiratory activity in the rat brainstem-spinal cord *in situ*: patterns, origins and implications for respiratory rhythm generation. J Physiol 587:3539–3559. CrossRef Medline

Amiel J, Dubreuil V, Ramanantsoa N, Fortin G, Gallego J, Brunet JF, Goridis C (2009) PHOX2B in respiratory control: lessons from congenital central hypoventilation syndrome and its mouse models. Respir Physiol Neurobiol 168:125–132. CrossRef Medline

Carroll MS, Patwari PP, Weese-Mayer DE (2010) Carbon dioxide chemoreception and hypoventilation syndromes with autonomic dysregulation. J Appl Physiol 108:979–988. CrossRef Medline

Corcoran AE, Richerson GB, Harris MB (2013) Serotonergic mechanisms are necessary for central respiratory chemoresponsiveness *in situ.* Respir Physiol Neurobiol 186:214–220. CrossRef Medline

Davis SE, Solhied G, Castillo M, Dwinell M, Brozoski D, Forster HV (2006) Postnatal developmental changes in CO2 sensitivity in rats. J Appl Physiol 101:1097–1103. CrossRef Medline

Dubreuil V, Ramanantsoa N, Trochet D, Vaubourg V, Amiel J, Gallego J, Brunet JF, Goridis C (2008) A human mutation in Phox2b causes lack of CO_2 chemosensitivity, fatal central apnea, and specific loss of parafacial neurons. Proc Natl Acad Sci U S A 105:1067–1072. CrossRef Medline

Dutschmann M, Wilson RJ, Paton JF (2000) Respiratory activity in neonatal rats. Auton Neurosci 84:19–29. CrossRef Medline

Feldman JL, Del Negro CA, Gray PA (2013) Understanding the rhythm of breathing: so near, yet so far. Annu Rev Physiol 75:423–452. CrossRef Medline

Gestreau C, Dutschmann M, Obled S, Bianchi AL (2005) Activation of XII motoneurons and premotor neurons during various oropharyngeal behaviors. Respir Physiol Neurobiol 147:159–176. CrossRef Medline

Gestreau C, Heitzmann D, Thomas J, Dubreuil V, Bandulik S, Reichold M, Bendahhou S, Pierson P, Sterner C, Peyronnet-Roux J, Benfriha C, Tegtmeier I, Ehnes H, Georgieff M, Lesage F, Brunet JF, Goridis C, Warth R, Barhanin J (2010) Task2 potassium channels set central respiratory CO_2 and O_2 sensitivity. Proc Natl Acad Sci U S A 107:2325–2330. CrossRef Medline

Guyenet PG, Stornetta RL, Bayliss DA (2010) Central respiratory chemoreception. J Comp Neurol 518:3883–3906. CrossRef Medline

Kanbar R, Stornetta RL, Cash DR, Lewis SJ, Guyenet PG (2010) Photostimulation of Phox2b medullary neurons activates cardiorespiratory function in conscious rats. Am J Respir Crit Care Med 182:1184–1194. CrossRef Medline

Kay AR, Wong RK (1986) Isolation of neurons suitable for patch-clamping from adult mammalian central nervous systems. J Neurosci Methods 16:227–238. CrossRef Medline

Lazarenko RM, Milner TA, Depuy SD, Stornetta RL, West GH, Kievits JA, Bayliss DA, Guyenet PG (2009) Acid sensitivity and ultrastructure of the retrotrapezoid nucleus in Phox2b-EGFP transgenic mice. J Comp Neurol 517:69–86. CrossRef Medline

Lazarenko RM, Fortuna MG, Shi Y, Mulkey DK, Takakura AC, Moreira TS, Guyenet PG, Bayliss DA (2010) Anesthetic activation of central respiratory chemoreceptor neurons involves inhibition of a THIK-1-like background K^+ current. J Neurosci 30:9324–9334. CrossRef Medline

Leighton PA, Mitchell KJ, Goodrich LV, Lu X, Pinson K, Scherz P, Skarnes WC, Tessier-Lavigne M (2001) Defining brain wiring patterns and mechanisms through gene trapping in mice. Nature 410:174–179. CrossRef Medline

Lesage F, Barhanin J (2011) Molecular physiology of pH-sensitive background K_{2P} channels. Physiology (Bethesda) 26:424–437. CrossRef

Marina N, Abdala AP, Trapp S, Li A, Nattie EE, Hewinson J, Smith JC, Paton JF, Gourine AV (2010) Essential role of Phox2b-expressing ventrolateral brainstem neurons in the chemosensory control of inspiration and expiration. J Neurosci 30:12466–12473. CrossRef Medline

Molkov YI, Zoccal DB, Moraes DJ, Paton JF, Machado BH, Rybak IA (2011) Intermittent hypoxia-induced sensitization of central chemoreceptors contributes to sympathetic nerve activity during late expiration in rats. J Neurophysiol 105:3080–3091. CrossRef Medline

Mulkey DK, Stornetta RL, Weston MC, Simmons JR, Parker A, Bayliss DA, Guyenet PG (2004) Respiratory control by ventral surface chemoreceptor neurons in rats. Nat Neurosci 7:1360–1369. CrossRef Medline

Mulkey DK, Talley EM, Stornetta RL, Siegel AR, West GH, Chen X, Sen N, Mistry AM, Guyenet PG, Bayliss DA (2007) TASK channels determine pH sensitivity in select respiratory neurons but do not contribute to central respiratory chemosensitivity. J Neurosci 27:14049–14058. CrossRef Medline

Nattie E, Li A (2006) Central chemoreception 2005: a brief review. Auton Neurosci 126–127:332–338.

Onimaru H, Ikeda K, Kawakami K (2012) Postsynaptic mechanisms of CO_2 responses in parafacial respiratory neurons of newborn rats. J Physiol 590:1615–1624. CrossRef Medline

Paton JF (1996) A working heart-brainstem preparation of the mouse. J Neurosci Methods 65:63–68. CrossRef Medline

Paxinos G, Franklin KBJ (2004) The mouse brain in stereotaxic coordinates. Amsterdam: Elsevier.

Perkins KL (2006) Cell-attached voltage-clamp and current-clamp recording and stimulation techniques in brain slices. J Neurosci Methods 154:1–18. CrossRef Medline

Putnam RW, Filosa JA, Ritucci NA (2004) Cellular mechanisms involved in CO_2 and acid signaling in chemosensitive neurons. Am J Physiol Cell Physiol 287:C1493–C1526. CrossRef Medline

Ramanantsoa N, Hirsch MR, Thoby-Brisson M, Dubreuil V, Bouvier J, Ruffault PL, Matrot B, Fortin G, Brunet JF, Gallego J, Goridis C (2011) Breathing without CO_2 chemosensitivity in conditional Phox2b mutants. J Neurosci 31:12880–12888. CrossRef Medline

Stettner GM, Zanella S, Huppke P, Gärtner J, Hilaire G, Dutschmann M (2008) Spontaneous central apneas occur in the C57BL/6J mouse strain. Respir Physiol Neurobiol 160:21–27. CrossRef Medline

Stornetta RL, Moreira TS, Takakura AC, Kang BJ, Chang DA, West GH, Brunet JF, Mulkey DK, Bayliss DA, Guyenet PG (2006) Expression of Phox2b by brainstem neurons involved in chemosensory integration in the adult rat. J Neurosci 26:10305–10314. CrossRef Medline

Stunden CE, Filosa JA, Garcia AJ, Dean JB, Putnam RW (2001) Development of *in vivo* ventilatory and single chemosensitive neuron responses to hypercapnia in rats. Respir Physiol 127:135–155. CrossRef Medline

Takakura AC, Moreira TS, Stornetta RL, West GH, Gwilt JM, Guyenet PG (2008) Selective lesion of retrotrapezoid Phox2b-expressing neurons raises the apnoeic threshold in rats. J Physiol 586:2975–2991. CrossRef Medline

Wang S, Shi Y, Shu S, Guyenet PG, Bayliss DA (2013) Phox2b-expressing retrotrapezoid neurons are intrinsically responsive to H^+ and CO_2. J Neurosci 33:7756–7761. CrossRef Medline

Warth R, Barrière H, Meneton P, Bloch M, Thomas J, Tauc M, Heitzmann D, Romeo E, Verrey F, Mengual R, Guy N, Bendahhou S, Lesage F, Poujeol P, Barhanin J (2004) Proximal renal tubular acidosis in TASK2 K^+ channel-deficient mice reveals a mechanism for stabilizing bicarbonate transport. Proc Natl Acad Sci U S A 101:8215–8220. CrossRef Medline

Wilson RJ, Remmers JE, Paton JF (2001) Brain stem PO_2 and pH of the working heart-brain stem preparation during vascular perfusion with aqueous medium. Am J Physiol Regul Integr Comp Physiol 281:R528–R538. Medline